Extension of the Hymostruc3D model for simulation of hydration and microstructure development of blended cements

Gao, Peng; Ye, Guang; Wei, Jiangxiong; Yu, Qijun

Publication date
2019

Document Version
Final published version

Published in
Heron

Extension of the Hymostruc3D model for simulation of hydration and microstructure development of blended cements

Peng Gao [1, 2], Guang Ye [1], Jiangxiong Wei [2], Qijun Yu [2]

[1] Microlab, Faculty of Civil Engineering and Geosciences, Delft University of Technology, Delft, the Netherlands

[2] School of Materials Science and Engineering, South China University of Technology, Guangzhou, People's Republic of China

The HYMOSTRUC3D model has been used successfully to predict hydration and microstructure development of pure Portland cement paste. In recent years, a number of numerical models were proposed for optimizing the use of supplementary cementitious materials. Also HYMOSTRUC3D was extended for simulating the hydration and microstructure development of Portland cement blended with blast furnace slag or/and fly ash (Gao, 2018). This paper summarises the main features of this extended model, called HYMOSTRUC3D-E, and demonstrates the simulation of the hydration process and pore solution chemistry of slag cements.

Key words: Simulation, blended cement, hydration, microstructure

1 Introduction

In 1991 Van Breugel (1991) proposed a numerical cement hydration model called HYMOSTRUC, the acronym for HYdration, MOrphology and STRUCture formation. In this model, cement particles were homogenously distributed in a 3D cell (Figure 1a). With progress of the hydration process, hydration products were formed on the surface of the shrinking cores of hydrating cement particles. The hydration process of cement particles was divided into two stages, viz., phase boundary reaction stage and diffusion-controlled reaction stage. During both stages the reaction rate of cement particles was calculated as a function of the chemical composition and particle size distribution of the cement, water content and temperature of the system.

HYMOSTRUC focused on simulating the hydration process of Portland cements. It also simulated the microstructure of cement pastes by distributing the cement particles homogenously in the 3D cell (Figure 1a). Using this 3D cell microstructure, the contact areas between hydrating cement particles were calculated. The calculated contact areas were used to predict the mechanical properties of cement paste, such as strength and stiffness.

Koenders (1997) incorporated an algorithm in HYMOSTRUC to simulate the random spatial distribution of cement particles in the representative elementary volume (REV) of cement paste (see Figure 1b). Ye (2003) incorporated a pixel-based algorithm in HYMOSTRUC to analyse the pores of the simulated microstructure. Since the extensions of HYMOSTRUC concentrated on the 3D microstructure simulation, the new version of HYMOSTRUC is called HYMOSTRUC3D.

HYMOSTRUC3D has successfully been used to predict many properties of cement-based materials, including autogenous shrinkage of cement pastes (Koenders, 1997), transport properties of cement pastes (Ye et al., 2006) and tensile strength and stiffness of cement pastes (Qian, 2010) etc.

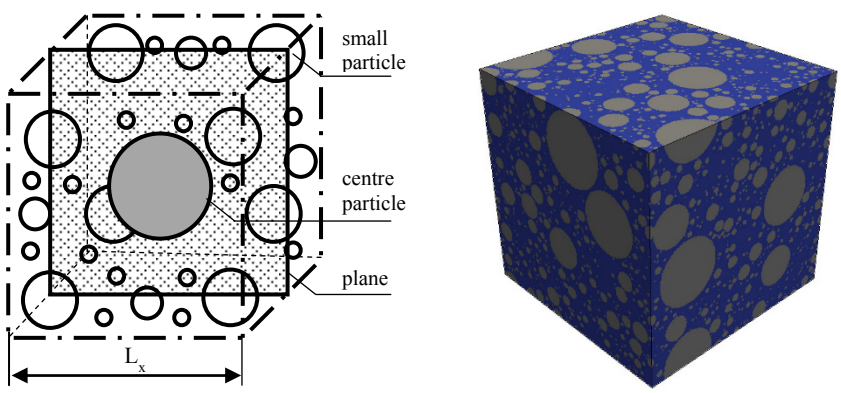

(a) homogenously distribution *(b) spatial distribution*

Figure 1: Average creep curves of nailed joints at 30%, 40% and 50% load level on a logarithmic time scale

Recently, there was much attention for numerical models for simulating hydration and microstructure of Portland cement (PC) blended with supplementary cementitious

materials (SCMs) such as blast furnace slag (BFS) and fly ash (FA). Also, the HYMOSTRUC3D model was extended for simulating the hydration and microstructure development of PC blended with BFS or/and FA (Gao, 2018). This model, called HYMOSTRUC3D-E, deals particularly with the pore solution chemistry of blended cement paste and its influence on the reaction of BFS or/and FA. The nucleation and growth of CH particles are simulated. In addition, a pore structure module was proposed to determine the porosity of capillary pores and gel pores of blended cement paste. This paper summarises the main features of the HYMOSTRUC3D-E model and demonstrates the simulation of the hydration process and pore solution chemistry of slag cements.

2 Structure of HYMOSTRUC3D-E

In a blended cement system, the dissolution of cementitious particles and the formation of hydration products are the two main processes of the hydration and microstructure development of blended cement. Several aspects of these two processes should be addressed for simulating the hydration and microstructure development of blended cement, including:

- Stoichiometry of the hydration of blended cement
- Kinetics of the reaction of blended cement
- Pore solution chemistry
- Interactions between PC, BFS and FA particles
- Multi-scale pore structure

To deal with the above aspects, several modules were proposed in the HYMOSTRUC3D-E model. As shown in Figure 2, these modules can be classified as two routes, viz. the *cement hydration route* and the *microstructure development route*.

*2.1 **Cement hydration route***

(1) Hydration module

The hydration module deals with the stoichiometry of the reactions in blended cement paste. The reaction rates of PC, including the clinker components of PC, BFS and FA, were calculated based on the assumptions that the reaction processes of these phases change from *phase boundary reaction* to *diffusion-controlled reaction*. The reaction rate of a PC particle was described with the formula:

$$\frac{\Delta\delta_{in,x_i,j+1,M_k}}{\Delta t_{j+1}} = K_{0,M_k} \times \Omega_1(\cdot) \times \Omega_2(\cdot) \times \Omega_3(\cdot) \times F_1(\cdot) \times \left[F_2(\cdot) \times \left(\frac{\delta_{tr,M_k}}{\delta_{x_i,j,M_k}} \right)^{\beta_1} \right]^{\lambda_{M_k}} \quad (1)$$

where $\Delta\delta_{in,x_i,j+1,M_k}$ is an incremental increase of the penetration depth of cement component M_k during a time increment $\Delta t_{j+1} = t_{j+1} - t_j$. $M_{k=1} = C_3S$, $M_{k=2} = C_2S$, $M_{k=3} = C_3A$, $M_{k=4} = C_4AF$. K_{0,M_k} is the initial penetration rate of the reaction front of hydrating cement component M_k [μm/hour]. Ω_1, Ω_2, Ω_3 are the reduction factors allowing for the change of water distribution and change in pore water chemistry in the system. F_1 represents the influence of temperature on the rate of reaction. F_2 accounts for the influence of temperature on the morphology and structure of hydration products. δ_{tr,M_k} is the transition thickness of the shell of hydration products when the hydration mechanism of M_k changes from *phase boundary reaction* to *diffusion-controlled reaction*. δ_{x_i,j,M_k} is the total thickness of inner product and outer product. λ_{M_k} is a coefficient to control reaction mechanisms (from *phase boundary reaction* ($\lambda_{M_k} = 0$) to *diffusion-controlled reaction* ($\lambda_{M_k} = 1$)). β_1 is a calibration parameter.

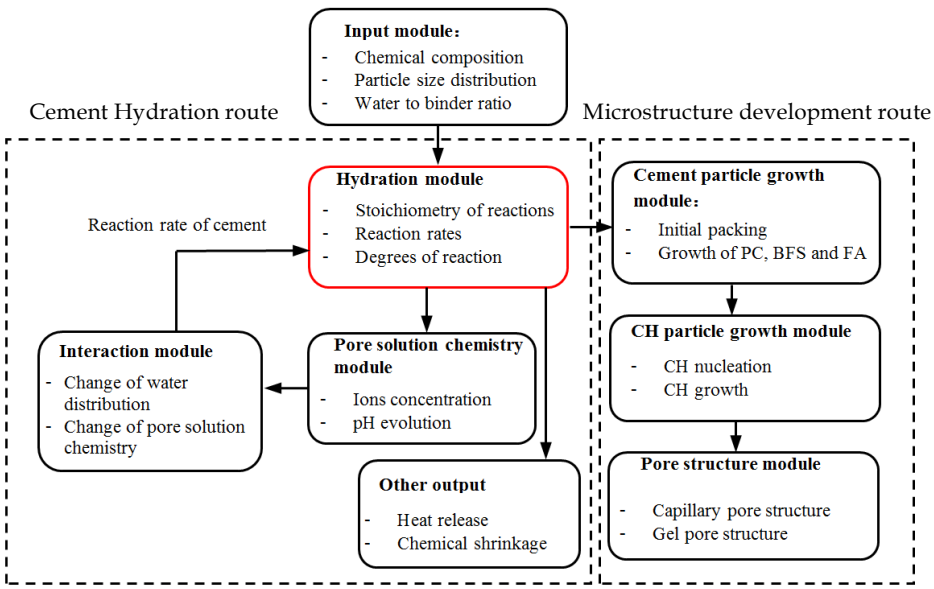

Figure 2: Structure of the HYMOSTRUC3D-E model

The reaction rate of a BFS or FA particle was described with the formula:

$$\frac{\Delta\delta_{in,x_i,j+1,S_k}}{\Delta t_{j+1}} = K_{0,S_k} \times \Omega_1(\cdot) \times \Omega_2(\cdot) \times \Omega_3(\cdot) \times F_1(\cdot) \times \left[F_2(\cdot) \times \left(\frac{\sigma_{tr,S_k}}{\delta_{x_i,j,S_k}} \right)^{\beta_1} \right]^{\lambda_{S_k}} \times M_{pH,S_k} \quad (2)$$

where $\Delta\delta_{in,x_i,j+1,S_k}$ is an incremental increase of the penetration depth of BFS or FA particle during a time increment $\Delta t_{j+1} = t_{j+1} - t_j$. $S_{k=1}$ = BFS, $S_{k=2}$ = FA. K_{0,S_k} is the initial penetration rate of the reaction part of BFS or FA [μm/hour], respectively. σ_{tr,S_k} is the transition thickness of the shell of hydration products when the hydration mechanism of BFS or FA particle changes from *phase boundary reaction* to *diffusion-controlled reaction*. M_{pH,S_k} represents the influence of pH on the reaction rate of BFS or FA.

The degrees of reactions of PC, BFS and FA were calculated from the reaction rates of these phases.

(2) Pore solution module

In the pore solution chemistry module, the calculated degrees of reactions of PC, BFS and FA were used to simulate the concentration of ions in the pore solution of blended cement paste. Five types of ions, i.e. Na^+, K^+, Ca^{2+}, SO_4^{2-} and OH^-, were involved. Other ions, such as $Al(OH)_4^-$ and $SiO(OH)_3^-$ were not incorporated because their concentrations are much less than of these five ions. Figure 3 shows the main steps in this module. Firstly, the volume of capillary water was calculated based on the evolution of phases in the cement paste. Then, the concentrations of Na^+ and K^+ ions were calculated based on Taylor's method (1987). Next, the concentrations of Ca^{2+}, SO_4^{2-} and OH^- ions were calculated with the solubility equilibria of CH and gypsum, and the electrical neutrality of pore solution.

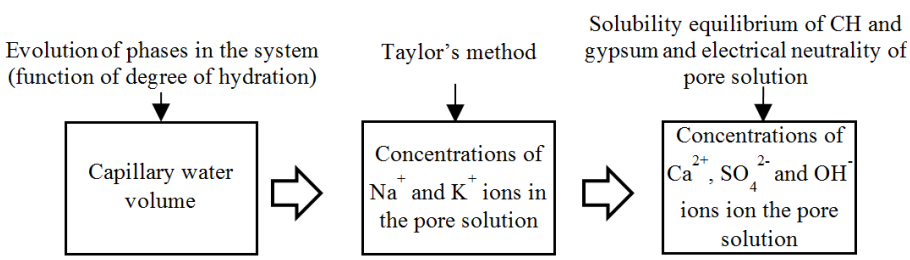

Figure 3: Main steps in the pore solution chemistry module

(3) Interaction module

In the interaction module, the effects of water distribution and the evolution of pore solution chemistry in the cement paste on the reactions of PC, BFS and FA were quantified. It is noted that different from the hydration of PC, both the reactions of BFS and FA are sensitive to the pore solution chemistry, particularly the pH value. Hence, to quantify the influence of pH value on the reactions of BFS and FA, a pH-factor M_{pH} was introduced (see Figure 4).

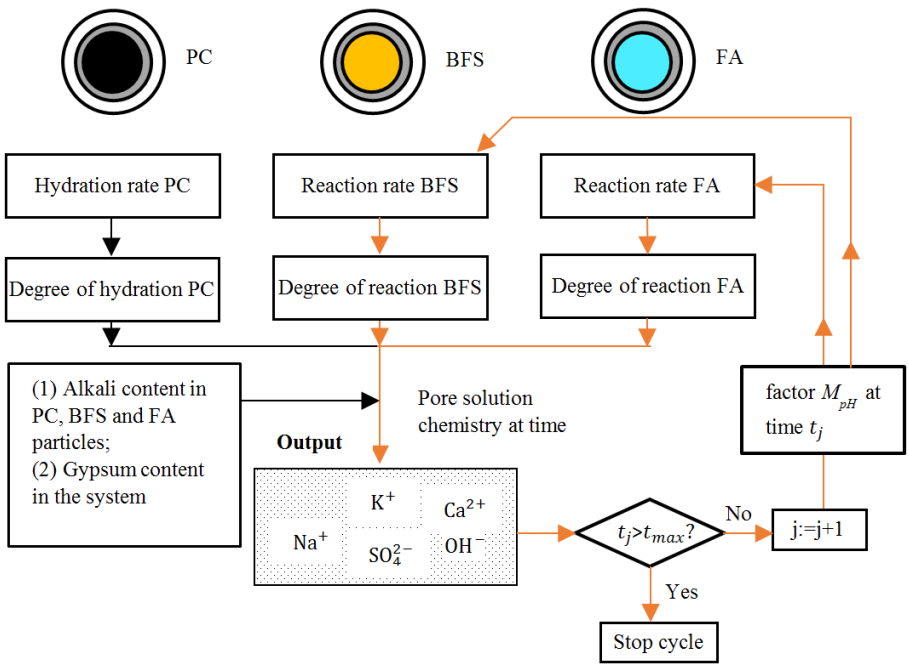

Figure 4: Schematic representation of the relationship between the pore solution chemistry, the factor M_{pH} and the reaction rate of BFS and FA. Note: The value of M_{pH} at time t = 0 is assumed to be 1. t_{max} is the maximum duration of the simulation period.

2.2 *Cement hydration route*

To simulate the microstructure development of blended cement paste, several phases were considered in HYMOSTRUC3D-E model:

- Unreacted PC, BFS and FA particles,
- Hydration products of PC: CSH gel and CH,
- Reactions products of BFS and FA: CSH gel,
- Pore space, including water and empty capillary pores

In addition, the CSH gel produced by the hydration of PC and the pozzolanic reactions of BFS and FA was subdivided in high density gel (inner product) and low density gel (outer product). Other hydration products, such as AFt and AFm phases, was considered as the part of CSH gel. Different from HYMOSTRUC3D, the CH produced during the hydration of PC was separated from the gel phase in HYMOSTRUC3D-E.

(1) Cement particle growth module

In the cement particle growth module, a REV of cement paste was built first. The initial spatial distribution of particles in the fresh paste was simulated by random packing of the PC, BFS and FA particles in the REV. In the packing algorithm, the particles with sizes from big to small were randomly placed, and no overlap existed between particles (see Figure 5). Then, by letting these PC, BFS and FA particles grow, the microstructure development of blended cement paste was simulated. In the algorithm for particle growth, the thickness of the shell of reaction product depended on the degree of hydration of the blended cement obtained in the cement hydration route.

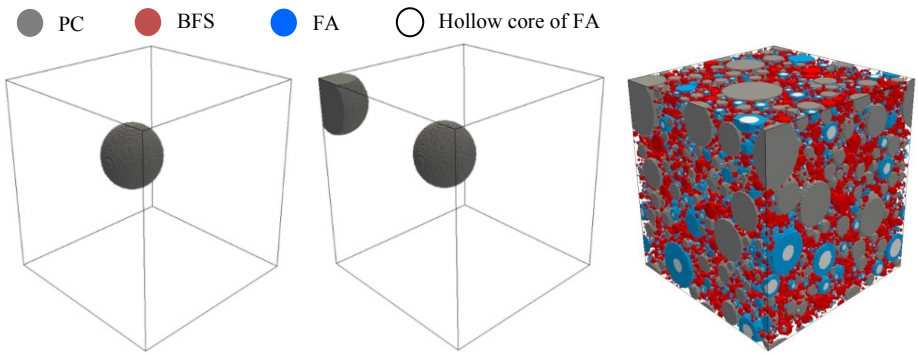

Figure 5: Schematic diagram of the random packing algorithm: (a) Largest PC particle was packed, (b) Second PC particle was packed, (c) All PC, BFS and FA particles were packed

(2) CH particle growth module

As reported by Gallucci et al. (2007), gypsum particles could also act as CH nuclei. In addition, increasing supersaturation ratio of Ca^{2+} and OH^- ions in the pore solution could form CH nuclei (Klein et al., 1968). Following the above two mechanisms, the number of CH nuclei was calculated as the number of gypsum particles (Eq. 3) and the supersaturation ratio in the pore solution (Eq. 4).

$$N_{gyp} = N_{PC} \times \frac{V_{gyp}}{V_{gyp} + V_{PC}} = N_{PC} \times \frac{\frac{f_{gyp}}{\rho_{gyp}}}{\frac{f_{gyp}}{\rho_{gyp}} + \frac{1 - f_{gyp}}{\rho_{PC}}} \quad (3)$$

$$\frac{dN_{CH}}{dt} = \frac{D_{Ca,OH}}{d_{CH}^2} v_0 \sqrt{\frac{2 \ln \frac{IP}{K_{sp,CH}}}{3\pi n^*}} \exp \frac{-\Delta G^*}{kT} \quad (4)$$

To simulate the growth of CH particles, a rule introduced by Scherer [2002] was used, viz. "*if there is a path connecting small and large pores, small crystals will dissolve and the solute will diffuse to a larger pore where the chemical potential of the crystal will be lower*". Figure 6 shows the schematic representation of the simulation of the growth process of CH particles in HYMOSTRUC3D-E.

(a) (b) (c)

Figure 6: Schematic representation of the growth of CH particles in HYMOSTRUC3D-E: (a) Placing CH nuclei in big pores to small pores; (b) Growth of CH nuclei in "biggest" pore; (c) Growth of other CH nuclei until the total volume in the 3D pore space ($V_1 + V_2 + V_3 + \ldots V_i$) has reached the volume of CH particles calculated based on the stoichiometry of cement hydration. Note: the number in (a) represents the sequence to place CH nuclei.

(3) Pore structure module

This pore structure module distinguishes three levels:

Level I: At the nanoscale, <5 nm, the concept of CSH globules proposed by Jennings (2000; 2004; 2008) was adopted. As shown in the right part of Figure 7, this CSH globule consisted of layers of CSH chains and interlayer water. The pore space between CSH chains were defined as interlayer gel pores.

Level II: Also at the nanoscale, but now in the range from 5 nm to 100 nm, the nanostructures of inner and outer CSH gels were determined by the packing of CSH globules, respectively (see the middle part of Figure 7). The packing density of inner CSH gels was higher than that of outer CSH gels. Gel pores were defined as the space between the CSH globules. The nanostructures of inner and outer CSH gels were assigned to the inner and outer products calculated with HYMOSTRUC3D-E.

Level III: At the microscale, from 100 nm to 100 µm, capillary pores form between solid phases (see the bottom part of Figure 7). It is noted that at this scale CSH gels were considered as one porous phase, consisting of inner and outer products.

3 Comparison between HYMOSTRUC3D and HYMOSTRUC3D-E

3.1 Reduction factors

HYMOSTRUC3D-E deals with the reactions of BFS and FA and their contribution to the microstructure formation. In addition, it refines the simulation of the hydration of PC, partially in calculating the hydration rate. In HYMOSTRUC3D, the reduction factors Ω_1 , Ω_2 and Ω_3 , allowing for the change of water distribution and change in pore water

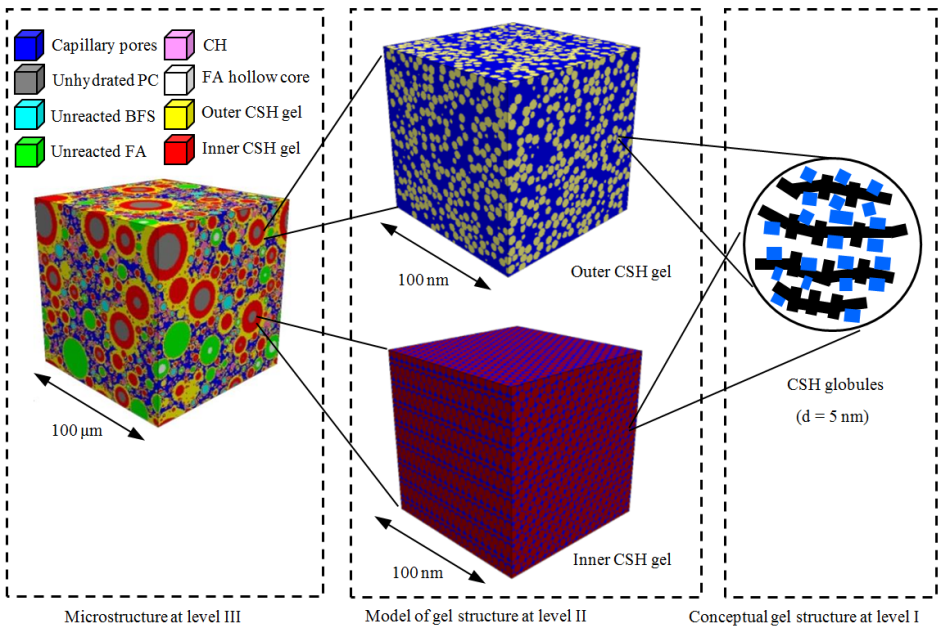

Figure 7: Pore structure module for blended cement paste

chemistry in the cement paste, are important for simulating the hydration rate of PC. In the following paragraphs the values of reduction factors Ω_1 , Ω_2 and Ω_3 HYMOSTRUC3D-E will be compared with the values used in the original HYMOSTRUC program.

(1) Reduction factor Ω_1

The reduction factor Ω_1 , allowing for the so called water withdrawal mechanism, affects the reaction rate of PC particles. The value of Ω_1 will be different for particles with different size. In this section the value of Ω_1 for PC particles with diameter = 40 μm was used for the comparison between HYMOSTRUC and HYMOSTRUC3D-E. Figure 8 shows the evolutions of reduction factor Ω_1 for the 40 μm PC particles in pure PC paste (w/c = 0.4) simulated with HYMOSTRUC and HYMOSTRUC3D-E. The value of Ω_1 simulated with HYMOSTRUC3D-E slightly differs from that simulated with HYMOSTRUC. This difference is caused by different values of the chemically bound water used in HYMOSTRUC3D-E and HYMOSTRUC. In HYMOSTRUC the chemically bound water for the hydration of PC was assumed to be 0.4 [g/g] (see Figure 9). In HYMOSTRUC3D-E the chemically bound water was calculated based on the stoichiometry of the hydration of the individual PC components. Because the stoichiometry of the hydration of PC changes with progress of the hydration process, the chemically bound water for the hydration PC [g/g] will also change in HYMOSTRUC3D-E. As shown in the black line of Figure 9, in HYMOSTRUC3D-E the value of the chemical bound water for the hydration of PC decreases from 0.55 [g/g] to 0.34 [g/g] and then increases to 0.38 [g/g].

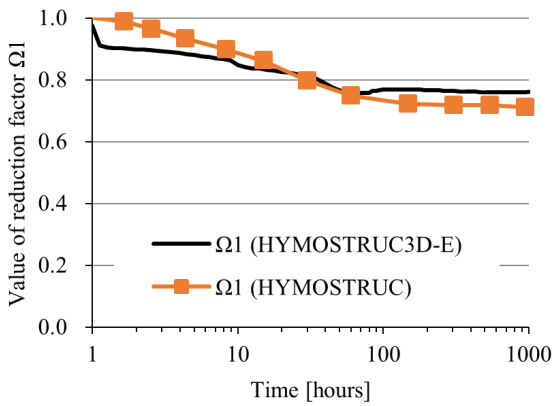

Figure 8: The evolution of reduction factor Ω_1 *simulated with HYMOSTRUC and HYMOSTRUC3D-E for the 40 μm PC particles in pure PC paste (w/c = 0.4)*

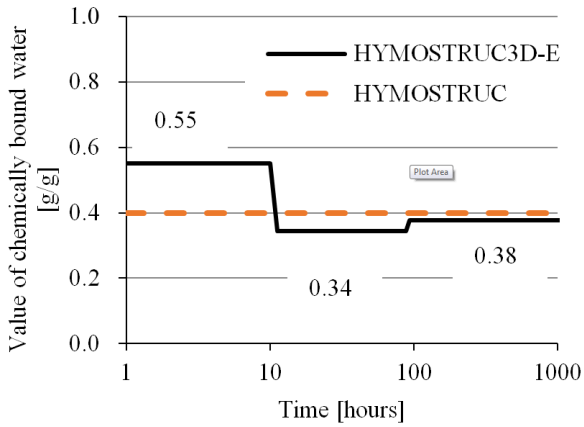

Figure 9: The evolutions of chemically bound water of the hydration of PC in HYMOSTRUC and HYMOSTRUC3D-E

(2) Reduction factor Ω_2

In both HYMOSTRUC and HYMOSTRUC3D-E, the reduction factor Ω_2 was used to quantify the influence of the water shortage in capillary pores on the reaction rate of PC particles. According to the concept of Ω_2 , the value of Ω_2 depends on the pore wall area of capillary pores filled with water $A_{wat}(\alpha)$ and the total capillary pore wall area $A_{por}(\alpha)$. Figure 10 shows the evolutions of the reduction factor Ω_2 in pure PC paste (w/c = 0.4) simulated with HYMOSTRUC and HYMOSTRUC3D-E. The value of Ω_2 simulated with HYMOSTRUC3D-E

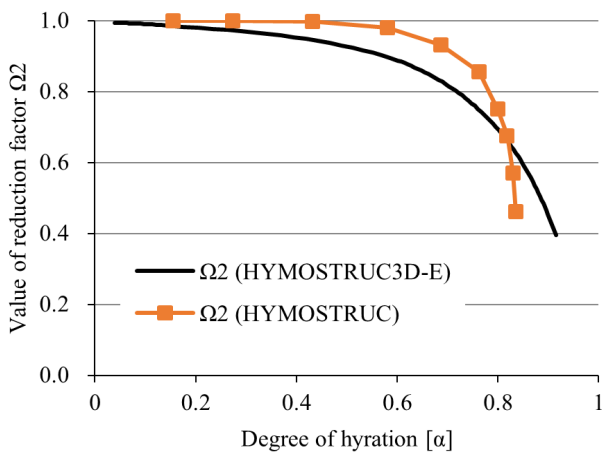

Figure 10: Evolution of Ω_2 *in PC paste (w/c = 0.4) simulated with HYMOSTRUC and HYMOSTRUC3D-E. Note: The thickness of the adsorption layer is 9 Å.*

slightly differs from that simulated with HYMOSTRUC. The difference between the values of Ω_2 in HYMOSTRUC and HYMOSTRUC3D-E has two reasons. The first reason is the difference in chemically bound water used in HYMOSTRUC3D-E and HYMOSTRUC (see Figure 10). The value of the chemically bound water will affect the amount of remaining capillary water and hence the value of $A_{wat}(\alpha)$. The second reason is the difference in pore structure simulated with HYMOSTRUC3D-E and HYMOSTRUC. The value of capillary pore volume $V_{por,j}$ will affect the values of both $A_{wat}(\alpha)$ and $A_{por}(\alpha)$. The value of Ω_2 in HYMOSTRUC3D-E is more realistic, as shown by the good agreement between the capillary porosity simulated with HYMOSTRUC3D-E and experimental results (Figure 11).

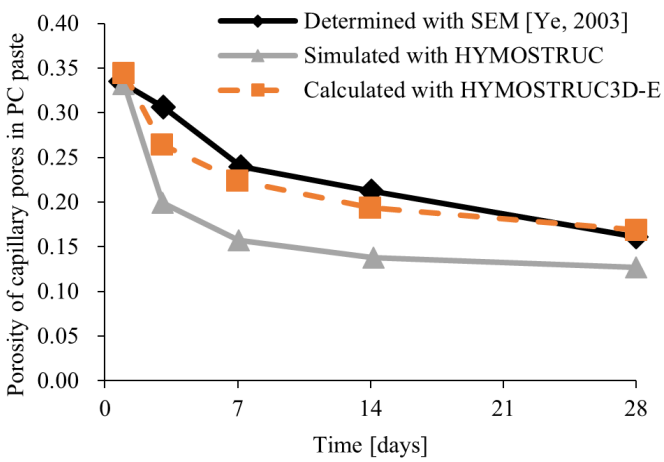

Figure 11: Porosity of capillary pores in PC paste (w/c = 0.4) simulated with HYMOSTRUC and HYMOSTRUC3D-E, and obtained with SEM

(3) Reduction factor Ω_3

In both HYMOSTRUC and HYMOSTRUC3D-E the reduction factor Ω_3 was used to quantify the influence of the total amount of Ca^{2+} ions accommodated in capillary water on the reaction rate of PC particles. Figure 12 shows the evolution of the reduction factor Ω_3 in a pure PC paste (w/c = 0.4) simulated with HYMOSTRUC and HYMOSTRUC3D-E. The value of Ω_3 simulated with HYMOSTRUC3D-E slightly differs from that simulated with HYMOSTRUC. This difference is also caused by the difference in amounts of chemically bound water used in HYMOSTRUC3D-E and HYMOSTRUC (Figure 12).

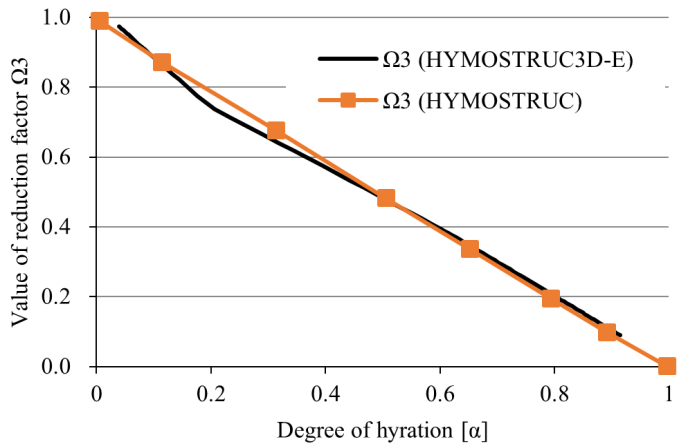

Figure 12: Evolution of Ω_3 in PC paste (w/c = 0.4) simulated with HYMOSTRUC and HYMOSTRUC3D-E

3.2 *Other features*

Table 1 lists the comparison between HYMOSTRUC3D and HYMOSTRUC3D-E. HYMOSTRU3D-E shows the following extensions:

(1) Blended systems

HYMOSTRUC3D was only able to simulate the hydration and microstructure development of pure PC system. HYMOSTRU3D-E was able to simulate the hydration and microstructure development of several systems: mono system (PC), binary system (PC blended with BFS or FA), ternary system (PC blended with BFS and FA).

(2) Pore solution chemistry

In HYMOSTRUC3D-E, the evolution of pore solution chemistry in cement paste was simulated, and the influence of the pore solution chemistry on the reaction rates of BFS and FA was quantified explicitly.

(3) Nucleation and growth of CH particles

HYMOSTRUC3D-E contained a module to simulate the nucleation and growth of CH particles.

(4) Evolution of gel porosity in cement paste

HYMOSTRU3D only gave the evolution of capillary porosity in cement paste. However, HYMOSTRU3D-E determined the evolution of the pore structure, including the

contribution of the gel pores to the total porosity of the cement paste. In this pore structure module, specific pore size distributions were assigned to the inner and outer products.

Table 1: Comparison between HYMOSTRUC3D and HYMOSTRUC3D-E

	HYMOSTRUC3D	HYMOSTRUC3D-E
Available systems	Mono system: PC paste	Mono system: PC paste Binary system: slag or fly ash cement paste Ternary system: PC blended with BFS and FA.
Degree of PC hydration	Available	Available
Degree of PC components	Available	Available
Microstructure	Available	Available
Pore solution chemistry	Unavailable	Available
Nucleation and growth of CH particles	Unavailable	Available
Evolution of capillary porosity in cement paste	Available	Available
Evolution of gel porosity in cement paste	Gel volume was already calculated	Specific pore size distributions are assigned to the inner and outer products.

4 Demonstration of the simulation of the hydration process and pore solution chemistry of slag cements

4.1 Input parameters

(1) Raw materials and mixture design

Table 2 lists the chemical compositions of PC and BFS. The mineral composition of PC calculated with the modified Bogue equation (Taylor, 1997) is: 63.6% C_3S, 9.7% C_2S, 7.3% C_3A and 9.7% C_4AF. The densities of PC and BFS are 3.15 g/cm^3 and 2.85 g/cm^3, respectively (Ye, 2006). As shown in Figure 13, the particle size distributions of PC and BFS follow the Rosin Rammler Bennett (RRB) distribution: $G(x) = 1 - \exp(-bx^n)$. $G(x)$ is the cumulative weight, x is the particle diameter, n and b are fitting parameters. Four mixtures will be considered. The mixture composition of pure PC and slag cement pastes are listed in Table 3.

Table 2: Chemical compositions of PC and BFS (Ye, 2006)

Raw materials	Chemical composition (wt. %)							
	CaO	SiO_2	Al_2O_3	Fe_2O_3	MgO	K_2O	Na_2O	SO_3
PC	64.1	20.1	4.8	3.2	0.0	0.52	0.28	2.7
BFS	40.8	35.4	13.0	0.53	8.0	0.49	0.21	0.1

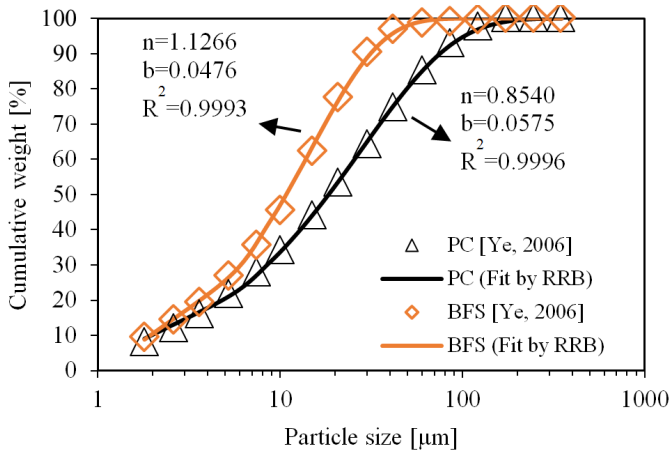

Figure 13: Particle size distribution of PC and BFS. The particle size distributions of PC and BFS follow Rosin Rammler Bennett (RRB) distribution

Table 3: Mixture proportions of slag cement pastes (Ye, 2006)

Sample No.	PC (wt. %)	BFS (wt. %)	w/b
P100B0-0.4	100	0	0.4
P70B30-0.4	70	30	0.4
P50B50-0.4	50	50	0.4
P30B70-0.4	30	70	0.4

(2) Model parameters

a. Hydration parameters K_0 and δ_{tr}

K_0 and δ_{tr} are two important model parameters. K_0 represents the initial penetration rate of the reaction front of hydrating PC-components or BFS. δ_{tr} is the transition thickness when the hydration mechanism of PC-components or BFS change from *phase boundary reaction* to *diffusion-controlled reaction*. The values of penetration rate K_0 and transition thickness δ_{tr} for PC-components and BFS are presented in Table 4.

Table 4: Obtained hydration parameters K_0 and δ_{tr} for different minerals of PC, and BFS particles

No.	Phase	K_0 [μm/hour]	δ_{tr} [μm]
1	C_3S	0.0705	2.65
2	C_2S	0.0051	3.11
3	C_3A	0.1329	3.50
4	C_4AF	0.0200	1.19
5	BFS	0.0045	0.19

b. Effect of pH on the reaction rate of BFS particles

In HYMOSTRU3D-E model the factor M_{pH} accounts for the effect of the pH on the dissolution rate of BFS particles (Eq. 5):

$$M_{pH,f,BFS} = 10^{A_{BFS}\times(pH_j - pH_{ref,BFS})} \tag{5}$$

where pH_j is the pH of the pore solution at time t_j . $pH_{ref,BFS}$ is the pH of the pore solution used to determine the initial penetration rate of the reaction front of a reacting BFS particle. A_{BFS} is the slope of the linear relationship between pH and the log dissolution of BFS. The value of A_{BFS} is set as 0.3 in the HYMOSTRUC3D-E model.

c. Binding factors of Na^+ and K^+ ions

The binding factors *b* in HYMOSTRUC3D-E model (Na^+ and K^+ bound by reaction products of PC and of blended cements) are important model parameters for simulating the pore solution chemistry. The values of binding factors *b* are listed in Table 5.

Table 5: Binding factors (Na^+ and K^+ bound by reaction products of PC (CSHPC and AFmPC) and of blended cements (CSHBFS and HTBFS) used in HYMOSTRUC3D-E

Ions	Binding factors [ml/g]			
	CSH_{PC}	AFm_{PC}	CSH_{BFS}	HT_{BFS}
Na^+	0.39	0.10	0.30	0.30
K^+	0.30	0.10	0.30	0.30

Note: CSH_{PC} and AFm_{PC} are the CSH and AFm produced by the hydration of PC, CSH_{BFS} and HT_{BFS} are the CSH and HT produced by the reaction of BFS.

d. Stoichiometry of the pozzolanic reaction of BFS

The stoichiometry of the pozzolanic reaction of BFS was described with Eq. (6)**Error! Reference source not found.**, which is from the research of Richardson et al. (2002):

$$C_{7.88}S_{7.39}M_3A + 2.6\ CH + 31.5\ H \rightarrow 7.39\ C_{1.42}SH_{2.92}A_{0.046} + 0.66\ M_{4.6}AH_{19} \quad (6)$$

where $C_{7.88}S_{7.39}M_3A$ represents BFS. $C_{1.42}SH_{2.92}A_{0.046}$ is the CSH gel produced in the reaction of BFS. $M_{4.6}AH_{19}$ is the hydrotalcite-like phase produced by the reaction of BFS.

4.2 *Degree of hydration or pozzolanic reaction*

(1) Degree of hydration of PC in pure PC and slag cement pastes (50 and 70% BFS)

Figure 14a shows the measured degree of hydration of PC in pure PC and in slag cement pastes using SEM (Ye, 2006). The experimental results show that the degree of hydration of PC is higher in the paste with higher BFS content. Because BFS reacts much slower than PC, there will be more space and more water for the hydration of PC in the paste with higher BFS content (Lothenbach et al., 2011).

Figure 14b shows the simulated degrees of hydration of PC in pure PC and in slag cement pastes. The simulated degrees of hydration of PC exhibit a trend similar to the experimental results. This trend (the addition of BFS increases the degree of hydration of PC) is simulated with the reduction factors Ω_1 , Ω_2 and Ω_3 , i.e. the factors that allow for the change of water distribution and change in pore water chemistry in the paste. If BFS is added in the paste, these reduction factors will be influenced.

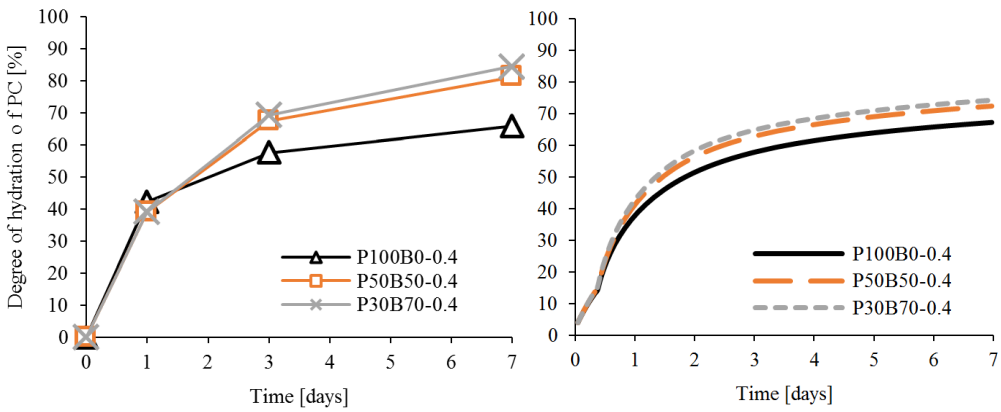

(a) Experimental results (Ye, 2006) *(b) Simulation with HYMOSTRUC3D-E*

Figure 14: Degree of hydration of PC in cement pastes with different BFS contents

(2) Degree of pozzolanic reaction of BFS in slag cement pastes

Figure 15a and Figure 15b show the degrees of pozzolanic reaction of BFS in slag cement pastes obtained by experiments and simulation, respectively. The simulations were performed with the function for simulating the reaction rate of BFS particles. The SEM results (Figure 15a) show that the degrees of pozzolanic reaction of BFS in P50B50 and P30B70 are close to each other. HYMOSTRUC3D-E model gives a similar trend (Figure 15b). In HYMOSTRUC3D-E model, the reaction rate of a BFS particle was not only described with the reduction factors Ω_1 , Ω_2 and Ω_3 allowing for the change of water distribution and change in pore water chemistry in the paste, but also depended on an additional factor M_{pH} for quantifying the effect of pH on the reaction rate of BFS.

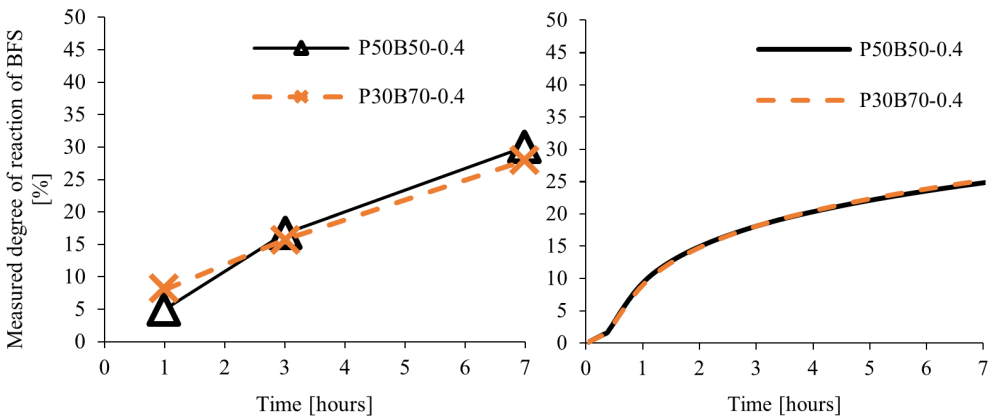

(a) Experimental results [Ye, 2006] *(b) Simulated with HYMOSTRUC3D-E*

Figure 15: Degree of pozzolanic reaction of BFS in binary systems

*4.3 **Pore solution chemistry***

(1) Concentrations of alkali ions

Figure 16a and Figure 17a show the measured concentrations of the alkali ions Na^+ and K^+ in the pore solution of PC and slag cement pastes (w/b = 0.4) up to 7 days, respectively. The concentrations of both Na^+ and K^+ ions increase with ongoing hydration. Besides, the cement paste with higher BFS content shows lower concentrations of Na^+ and K^+ ions. In general, the alkali ions in the pore solution are continuously released from the PC and BFS particles with progress of the hydration process. Because PC reacts much faster than BFS, the alkali ions in the pore solution mainly come from the dissolution of PC. Hence, the concentrations of alkali ions in the pore solution will be lower in the paste with higher BFS content.

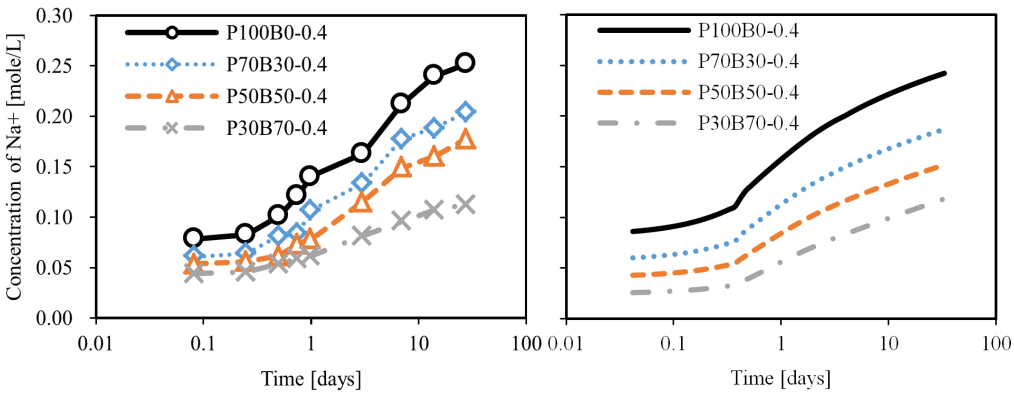

(a) measured Na^+ from Ye (2006) *(b) Na^+ simulated with HYMOSTRUC3D-E*

Figure 16: Concentrations of Na^+ ions in pore solutions of PC and slag cement pastes

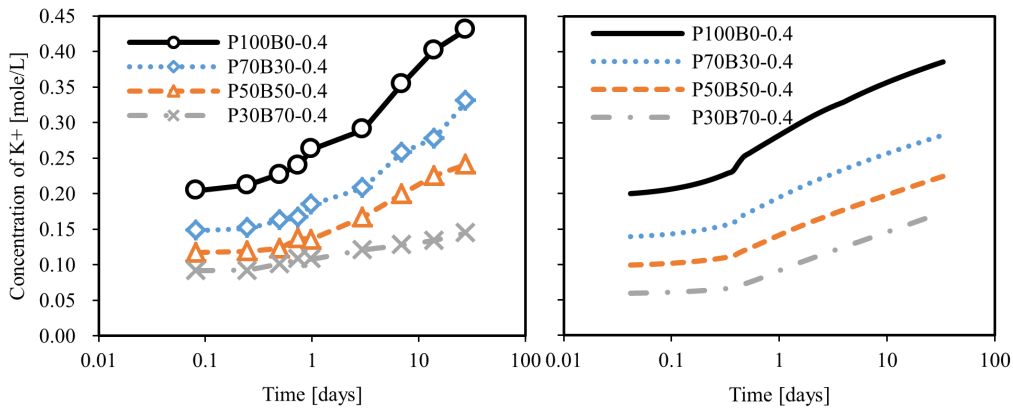

(a) measured K^+ from Ye (2006) *(b) K^+ simulated with HYMOSTRUC3D-E*

Figure 17: Concentrations of K^+ ions in pore solutions of PC and slag cement pastes

Figure 16b and Figure 17b show the simulated concentrations of Na^+ and K^+, respectively. The simulated evolutions of the concentrations of Na^+ and K^+ are close to the experimental data.

(2) Concentrations of Ca^{2+}

Figure 18a and Figure 18b show the concentrations of Ca^{2+} in the pore solution of PC and slag cement pastes obtained with experiments and HYMOSTRUC3D-E model, respectively. It is found that:

a. The concentration of Ca^{2+} decreases with time

With ongoing hydration, the concentrations of OH^- will increase because the concentrations of alkali ions will increase. According to the solubility equilibrium of CH, the concentration of Ca^{2+} will decrease if the concentration of OH^- increases. Besides, the concentrations of Ca^{2+} and SO_4^{2-} reach the solubility equilibrium of gypsum at very early age. This solubility equilibrium will also affect the concentration of Ca^{2+}. When gypsum is used up (after around 10 hours), the concentration of Ca^{2+} mainly depends on by the solubility equilibrium of CH. Both the results of experiments and simulations (Figure 18a and Figure 18b) show that the concentration of Ca^{2+} dramatically decreases at the moment the gypsum is used up.

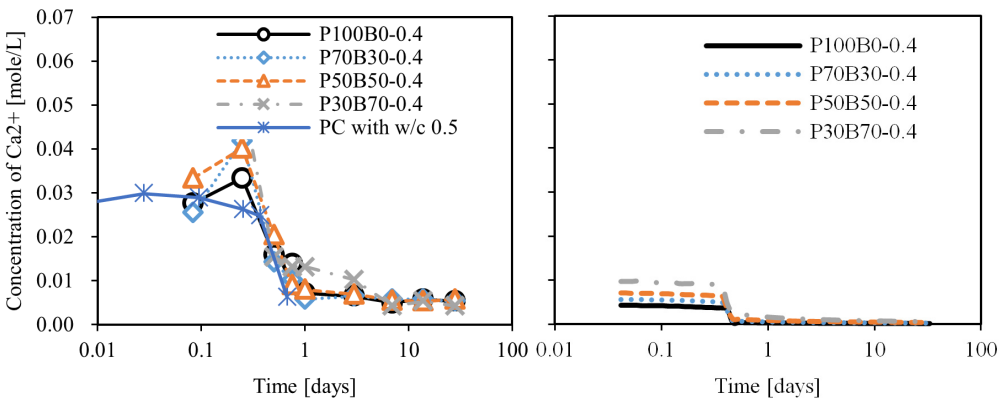

(a) measured Ca^{2+} from Ye (2006) *(b) Ca^{2+} simulated with HYMOSTRUC3D-E*

Figure 18: Concentrations of Ca^{2+} ions in the pore solutions of PC and slag cement pastes. Note: PC with w/c = 0.5 is the experimental data summarized in Taylor (1997)

b. The concentration of Ca^{2+} in BFS mixtures

As mentioned in the previous paragraph, the concentration of Ca^{2+} will decrease if the concentration of OH^- increases according to the solubility equilibrium of CH. The concentration of OH^- in the pore solution of cement-based materials mainly depends on the concentration of alkali ions. Because the concentration of alkali ions is lower in the paste with higher BFS content (see Figure 16 and Figure 17), the paste with higher BFS content will exhibit lower a concentration of OH^- and higher concentration of Ca^{2+}.

c. Simulated concentrations of Ca^{2+} are lower than the experimental data

The simulated concentrations of Ca^{2+} for the cement paste with a certain BFS content

(Figure 18b) are lower than experimental data (Figure 18a). There are two possible reasons for this. First, the actual Ca^{2+} and OH^- ions in pore solution are supersaturated at early age, which cannot be accurately calculated with *only* the concept of solubility equilibrium. Another possible reason is from inadequate consideration of the solubility equilibria of hydration products containing calcium. In HYMOSTRUC3D-E model it was assumed that the concentration of Ca^{2+} ions *only* depends on the solubility equilibria of gypsum and CH. In reality, the concentration of Ca^{2+} ions is also affected by the solubility equilibria of other phases in the cement paste, such as AFt, AFm, CSH.

(3) Concentrations of SO_4^{2-}

Figure 19a and Figure 19b show the concentrations of SO_4^{2-} in the pore solution of PC and slag cement pastes obtained by experiments and HYMOSTRUC3D-E, respectively. In the pore solution of cement paste the concentration of SO_4^{2-} ions mainly depends on the solubility equilibrium of gypsum. With ongoing hydration, the gypsum is gradually consumed by the hydration of the components of PC, C_3A and C_4AF. As a consequence, the concentration of SO_4^{2-} decreases with ongoing hydration. For the system with higher BFS content, the gypsum content is smaller. As a result, the concentration of SO_4^{2-} will become lower. As shown in Figure 19b, the simulated concentration of SO_4^{2-} exhibits a sharp decline after 10 hours. In HYMOSTRUC3D-E it was assumed that the SO_4^{2-} ions are *only* released from the dissolution of gypsum. After 10 hours the gypsum is used up by hydration of the components of PC, C_3A and C_4AF. Hence, the concentration of SO_4^{2-} will

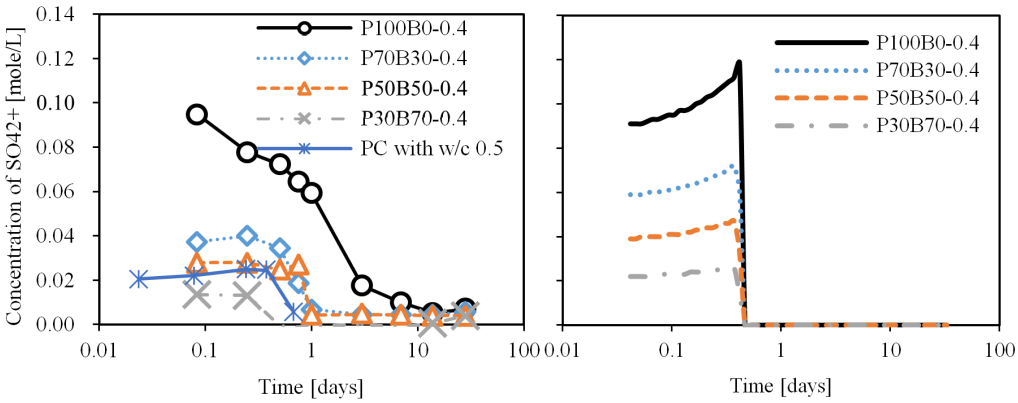

(a) measured SO_4^{2-} from Ye (2006) *(b) SO_4^{2-} simulated with HYMOSTRUC3D-E*

Figure 19: Concentrations of SO_4^{2-} ions in pore solutions of PC and slag cement pastes

Note: PC with w/c = 0.5 is the experimental data summarized in Taylor (1997)

decrease to zero. In reality the concentration of SO_4^{2-} ions is also related to the solubility equilibria of hydration products, such as AFt and AFm. As a result, the measured concentration of SO_4^{2-} will not completely decrease to zero, as shown in Figure 19a.

(4) Evolution of pH

Figure 20a and Figure 20b show the evolutions of pH in the pore solution of PC and slag cement pastes obtained with experiments and HYMOSTRUC3D-E, respectively. According to the experimental data (Figure 20a), the value of pH in the pore solution of blended cement pastes is lower in the paste with higher BFS content. The simulated evolution of the pH in the pore solution (Figure 20b) shows a sharp increase at around 10 hours. In the experiments a more gradual increase is observed. Except the difference in mode of change from low to high pH after about 0.5 to 1 days, the simulated evolution of the pH in the pore solution shows a trend similar to the experimental data.

5 Conclusions

(1) This paper presents the main features of HYMOSTRUC3D-E model. To simulate the hydration and microstructure development of blended cements, two hydration routes were followed: the *cement hydration route* and the *microstructure development route*. In the *cement hydration route*, a hydration module was proposed to deal with the stoichiometry, rates and degrees of the reactions of PC, BFS and FA. A pore solution chemistry module was proposed to quantify the evolution of the concentrations of Na^+, K^+, Ca^{2+}, SO_4^{2-} and OH^- ions and pH in the pore solution. Next, an interaction model was proposed to quantify

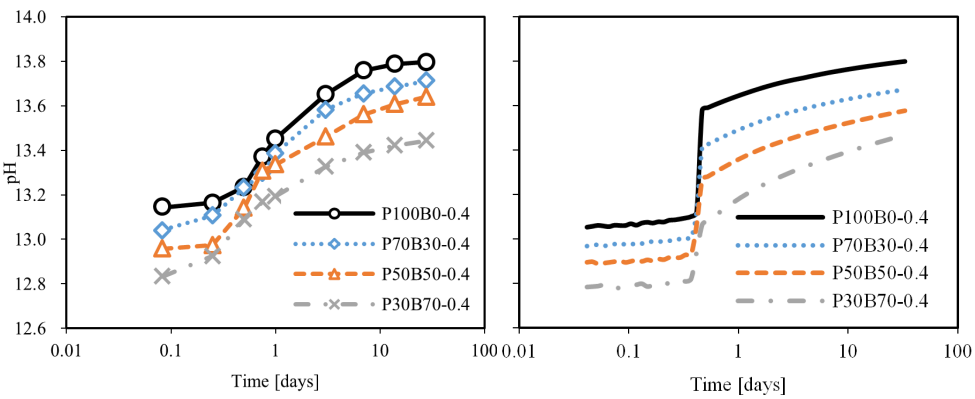

(a) measured pH from Ye (2006) *(b) pH simulated with HYMOSTRUC3D-E*

Figure 20: Evolution of pH in the pore solutions of PC and slag cement pastes

the influence of the change of water distribution and pore solution chemistry on the reaction rates of PC, BFS and FA. The *microstructure development route* consists of the cement particle growth module, the CH particle growth module and the pore structure model. In the cement particle growth module, a REV of cement paste was built first. Next, the initial spatial distribution of particles in the fresh paste was simulated by random packing of the PC, BFS and FA particles in the REV. Then, by letting these PC, BFS and FA particles grow, the microstructure development of blended cement paste was simulated. In the algorithm for particle growth, the thickness of the shell of the reaction product depends on the degree of hydration of the blended cement obtained in the *cement hydration route*. In the CH particle growth module, the nucleation and growth of CH particles in the pore space were simulated. In the pore structure module, the evolutions of capillary pores and gel pores in cement paste were determined.

(2) The hydration and pore solution chemistry of slag cements (w/b = 0.4, BFS content up to 70%) was simulated with the HYMOSTRUC3D-E model. The simulated degree of hydration of slag cements is in good agreement with experimental data of Ye (2006). The simulated concentrations of alkali ions (Na^+ and K^+) in the pore solution of slag cement pastes are close to the experimentally obtained data. The simulated concentrations of Ca^{2+} and SO_4^{2-} differ from the results of experiments, probably because the actual Ca^{2+} and OH^- ions in pore solution are supersaturated at an early age, which cannot be accurately calculated with *only* the concept of solubility equilibrium. Another possible reason for this is the actual concentrations of Ca^{2+} and SO_4^{2-} ions is also affected by the solubility equilibria of other phases in the cement paste, such as AFt, AFm, CSH. The simulated evolution of the pH of the pore solution shows a trend similar to the experimental results. This is because the concentrations of Ca^{2+} and SO_4^{2-} are much lower than those of alkali ions. The relatively low accuracy of the simulated concentrations of Ca^{2+} and SO_4^{2-} did not significantly influence the accuracy of the simulated evolution of the pH.

Acknowledgements

This work was funded by National key research and development program (2017YFB0310001-02), the National Natural Science Foundation of China (Grant No. 51672084 and 51772103), the China Postdoctoral Science Foundation funded project (Grant No. 2019M650199), China Scholarship Council (CSC), the doctoral visiting scholar program of South China University of Technology, and Research Centre of TU Delft in Urban System and Environment (No. C36103).

Literature

Gallucci, E. and Scrivener, K. (2007). Crystallisation of calcium hydroxide in early age model and ordinary cementitious systems. *Cement and Concrete Research*, 37(4): 492-501.

Gao, P., *Simulation of hydration and microstructure development of blended cements*. Ph.D. thesis, Delft University of Technology, the Netherlands, 2018.

Klein, D.H. and Smith, M.D. (1968). Homogeneous nucleation of calcium hydroxide. *Talanta*, 15(2), 229-231.

Koenders, E.A.B., *Simulation of volume changes in hardening cement-based materials*. Ph.D. thesis, Delft University of Technology, the Netherlands, 1997.

Lothenbach, B., Scrivener, K. and Hooton, R.D. (2011). Supplementary cementitious materials. *Cement and Concrete Research*, 41(12): 1244-1256.

Qian, Z., Schlangen, E., Ye, G. and Van Breugel, K. (2010). Prediction of mechanical properties of cement paste at microscale. *Materiales de Construcción*, 60 (297): 7-18.

Richardson, J.M., Biernacki, J.J., Stutzman, P.E. and Bentz, D.P. (2002). Stoichiometry of slag hydration with calcium hydroxide. *Journal of the American Ceramic Society*, 85(4): 947-953.

Scherer, G.W. (2002). Factors affecting crystallization pressure. In: International RILEM TC 186-ISA Workshop on Internal Sulfate Attack and Delayed Ettringite Formation, Villars, Switzerland, September, 139-154.

Taylor, H.F.W. (1987). A method for predicting alkali ion concentrations in cement pore solutions. *Advances in Cement Research*, 1(1): 5-17.

Taylor, H.F.W. Cement Chemistry. 2nd ed. London: Thomas Telford Publishing, 1997.

Van Breugel, K., *Simulation of hydration and formation of structure in hardening cement-based materials*. Ph.D. thesis, Delft University of Technology, the Netherlands, 1991.

Ye, G., *Experimental Study and Numerical Simulation of the Development of the microstructure and permeability of cementitious materials*, Ph.D. thesis, Delft University of Technology, the Netherlands, 2003.

Ye, G. Numerical simulation of connectivity of individual phases in hardening cement-based systems made of blended cement with and without admixtures, VENI report, Delft University of Technology, 2006.

Ye, G., Lura, P., Van Breugel, K. (2006). Modelling of water permeability in cementitious materials. *Materials & Structures*, 39(9):877-885.